Thermal resistance network model for heat conduction of amorphous polymers

Jun Zhou [1], Qing Xi,[1] Jixiong He,[2] Xiangfan Xu,[1] Tsuneyoshi Nakayama,[1,3] Yuanyuan Wang,[4,*] and Jun Liu [2,†]

[1]*Center for Phononics and Thermal Energy Science, China-EU Joint Lab for Nanophononics, School of Physics Science and Engineering, Tongji University, Shanghai 200092, China*
[2]*Department of Mechanical and Aerospace Engineering, North Carolina State University, Raleigh, North Carolina 27695, USA*
[3]*Department of Applied Physics, Hokkaido University, Sapporo, Hokkaido 060-0826, Japan*
[4]*School of Environmental and Materials Engineering, Shanghai Polytechnic University, Shanghai 201209, China*

The thermal conductivities (TCs) of the vast majority of amorphous polymers are in a very narrow range, 0.1–0.5 W m^{-1} K^{-1}, although single polymer chains possess TCs of orders of magnitude higher. The chemical structure of polymer chains plays an important role in determining the TC of bulk polymers. We propose a thermal resistance network (TRN) model for the TC in amorphous polymers taking into account the chemical structure of molecular chains. Our model elucidates the physical origin of the low TC universally observed in amorphous polymers with various chemical structures. The empirical formulas of the pressure and temperature dependence of TC can be successfully reproduced not only in solid polymers but also in polymer melts. We further quantitatively explain the anisotropic TC in oriented polymers.

I. INTRODUCTION

Polymers are ubiquitous in a wide range of applications from structure materials to electronics due to their diverse functionality, light weight, low cost, and chemical stability. The low thermal conductivity (TC) of polymers is a major technological barrier for the reliability and performance of polymer-based electronics due to a limited heat spreading capability. The TC of amorphous polymers is universally confined in a very narrow range, 0.1–0.5 W m^{-1} K^{-1} [1]. This feature indicates the possible existence of a universal thermal transport mechanism in amorphous polymers regardless of their distinct chemical structures [2]. Cahill *et al.* [3,4] have developed and tested a minimum thermal conductivity model for amorphous polymers, where sound velocity and atomic density govern the TC. Kommandur *et al.* [5] have developed an empirical model to predict the temperature-dependent TC of amorphous polymers, where density, monomer molecular weight, and velocity govern the dependence. All these models use bulk properties as inputs, which lack molecular chain details and thus are not able to describe the dependence of TC on temperature, pressure, and orientation, simultaneously.

An amorphous polymer is a three-dimensional (3D) van der Waals (vdW) solid formed by entangled, long, one-dimensional (1D) molecular chains [6]. Molecular dynamics (MD) simulations suggested that a single molecular chain may have a very high TC of orders of magnitude higher than its amorphous counterpart [7,8]. This difference is attributed to the fundamental distinction between the 1D chain and 3D network. A theoretical model for the TC of an amorphous polymer considering the microscopic structure of a 3D

network is highly desirable. Both intrachain and interchain thermal transport should be incorporated, where the intrachain thermal transport through a covalent bond is more efficient than the interchain thermal transport via vdW interactions.

In this paper, we propose a thermal resistance network (TRN) model for the TC of amorphous polymers, considering the interplay of interchain and intrachain thermal transport. Our model successfully identifies the physical reason for very low TCs and their relations with chemical structures in various amorphous polymers. Widely employed empirical relations on the temperature and pressure dependence of TCs can be reproduced from our model not only in solid polymers but also in polymer melts. Furthermore, this model is applicable to explain the anisotropic TC in oriented polymer nanofibers.

II. THERMAL RESISTANCE NETWORK MODEL

Figure 1(a) shows a unit box at a mesoscopic scale with entangled molecular chains that form a random isotropic network. We consider a heat current J that flows along the temperature gradient. The contact points of polymer chains are also illustrated. When heat flows across this network, the overall TRN is composed of three basic elements of resistors: (1) R_{intrin} is the average thermal resistance when heat flows through a chain segment between two adjacent contact points; (2) R_{intra} is the average thermal resistance when heat flows across a point and maintains in the same chain, i.e., intrachain resistance; and (3) R_{inter} is the average interfacial thermal resistance when heat flows across a point from one chain to another, i.e., interchain resistance. A typical trajectory of heat current is shown in Fig. 1(a) by solid lines. Heat flows from point 1 to point 2, up to point N. Segment (1,2) belongs to chain a, segments (2,3) and (3,4) belong to chain b, and segment (4,5) belongs to chain c. Therefore, heat flows from chain a to chain b via point 2 and from chain b to chain c

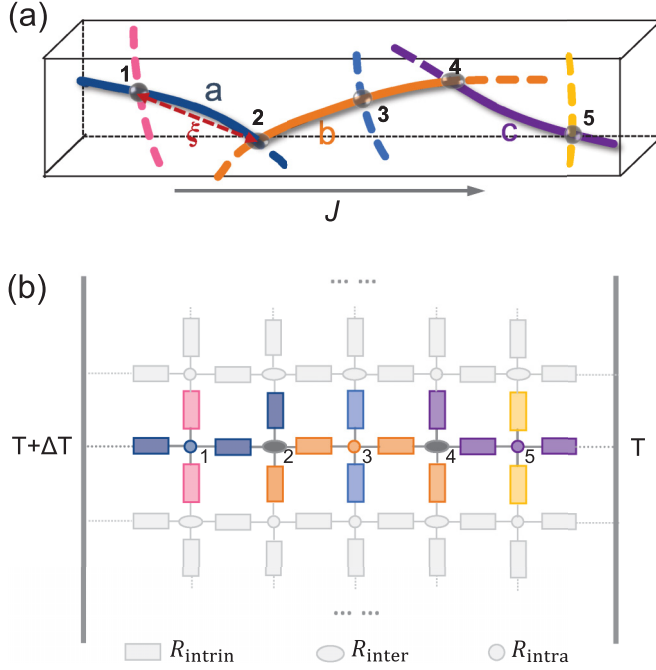*wangyuanyuan@sspu.edu.cn
†jliu38@ncsu.edu

FIG. 1. (a) Illustration of a representative unit of an amorphous polymer. Molecular chains are entangled, forming a network structure. The dominant heat flow trajectory is marked by solid lines where different colors are used for distinguishing chains. Contact points are labeled from 1 to 5 in the trajectory. (b) Topologically equivalent 2D TRN corresponding to the trajectory from 1 to 5 shown in (a). Rectangles, circles, and ellipses denote the intrinsic resistance of segments, intrachain resistance at the contact points, and interchain resistance, respectively.

via point 4. A topologically equivalent TRN, which is two dimensional (2D), is shown in Fig. 1(b). The overall thermal resistance R along the trajectory can be obtained by summing up all the resistance in a series,

$$R = N_{inter}R_{inter} + (N - N_{inter})R_{intra} + NR_{intrin}, \qquad (1)$$

where N_{inter} is the average number of interchain heat transfers, $R_{intrin} = \frac{\xi}{S\kappa_0}$ (K/W), ξ is the mean distance between two adjacent points, and κ_0 and S are the intrinsic TCs and cross sections of polymer chains, respectively. Taking polyethylene (PE) as an example, S is approximately 18 Å² [7] and the simulated κ_0 is 10–100 W m^{-1} K^{-1} [7–10]. Then the general form of TC of an isotropic d-dimensional polymer system ($d = 2, 3$) is

$$\kappa = \frac{1}{L^{d-2}} \frac{N^{d-1}}{R}$$

$$= \frac{1}{(\xi\overline{\cos\theta})^{d-2}[\gamma R_{inter} + (1 - \gamma)R_{intra} + R_{intrin}]}, \qquad (2)$$

where the size of system $L = \xi \sum_{i=1}^{N} \cos\theta_{i,i+1} \approx N\xi\overline{\cos\theta}$, $\theta_{i,i+1}$ is the angle between the axis and segment $(i, i+1)$, and $\overline{\cos\theta}$ is its average value. $\gamma = N_{inter}/N$ is the probability of interchain heat transfer. ξ could be calculated as

$$\xi = \left[\frac{2M_0}{a_0(\overline{\cos\theta})^d \rho}\right]^{\frac{1}{d-1}}. \qquad (3)$$

TABLE I. Structure parameters and TCs of typical amorphous polymers. N_A is the Avogadro constant, ρ and M_0 are from Ref. [16], and a_0 is from Refs. [16,19,20].

Polymers	ρ (g cm^{-3})	a_0 (Å)	$M_0 \times N_A$ (g mol^{-1})	ξ (Å)	κ_{am} (W m^{-1} K^{-1})
LDPE	0.855	1.27	14.0	18.5	0.16–0.48 [17]
PI	1.42	16.0	382.0	21.1	0.12 [16]
PT	1.4–1.6	7.8	194.0	21.0	0.17–0.21 [12]
N11	1.01	15.0	183.0	17.9	0.19 [16]
POM	1.42	1.93	30.0	17.1	0.16 [17]
PP	0.85	2.17	42.1	24.6	0.17 [17]
PVA	1.23–1.33	2.52	44.0	19.4	0.2 [16]
N6	0.6–0.7	8.6	113.2	24.1	0.23 [16]
PEEK	1.26	10.0	288.3	24.6	0.25 [16]
PET	1.41	10.76	192.0	18.3	0.22 [17]
N12	1.01–1.02	16.0	198.0	18.0	0.24 [16]
N66	1.14	17.2	226.3	17.5	0.25 [18]
N-alkane	0.66–0.79 [21]	1.27	14.0		0.123–0.153 [22]

ρ is the mass density, and M_0 and a_0 are the molecular weight and length of the repeating unit, respectively.

III. RESULTS AND DISCUSSIONS

Our model is valid for both 2D and 3D polymer systems and we focus on the 3D ones in this work. For isotropic polymers, $\overline{\cos\theta} = 1/2$, thus $\xi = 4\sqrt{M_0/(a_0\rho)}$. The probabilities of interchain and intrachain heat transfer at the contact points are the same. Therefore, we can take $\gamma = 1/2$ without loss of generality. In this case, R_{intra} and R_{intrin} are negligibly small compared with R_{inter}, which is on the order of 10 K nW^{-1} according to the MD simulations, because the interchain vdW interaction and/or hydrogen bond is much weaker than the covalent bond along individual chains. As a result, Eq. (2) can be expressed by the following neat form,

$$\kappa_{am} \approx \frac{4}{\xi R_{inter}} = \sqrt{\frac{\rho a_0}{M_0}} \frac{1}{R_{inter}}. \qquad (4)$$

We evaluate ξ of different polymers in Table I: branched low-density PE (LDPE), polyimide (PI), polythiophene (PT), Nylon-11 (N11), poly(oxymethylene) (POM), polypropylene (PP), poly(vinyl alcohol) (PVA), Nylon-6 (N6), poly(ether ether ketone) (PEEK), poly(ethylene terephthalate) (PET), Nylon-12 (N12), and Nylon-66 (N66). N-alkanes in their liquid state are also given for comparison. Calculated TCs vs $4/\xi$ are shown in Fig. 2(a) in comparison with experimental data [11–18]. We find that ξ ($4/\xi$) lies in a narrow range, 17.1–24.6 Å (0.16–0.23 Å^{-1}). Then the value of the TCs can be explained by choosing R_{inter} to be 6.5–16 K nW^{-1} near room temperature. Especially, the TCs of most polymers can be obtained by taking $R_{inter} \sim 10$ K nW^{-1}. This is because R_{inter} mainly comes from the vdW interactions whose strength should be similar in different polymers.

We further testify R_{inter} of PE and PP by means of MD simulations as shown in Fig. 2(b). We use the condensed-phase optimized molecular potentials for the atomistic simulation studies (COMPASS) force field to describe the interactive
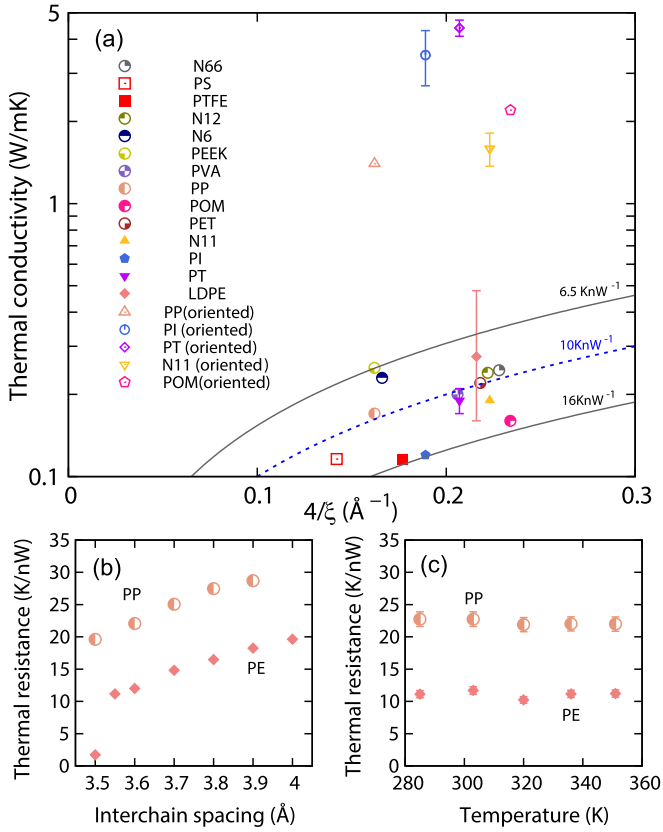
FIG. 2. (a) Calculated TCs vs $4/\xi$ using Eq. (4) with three different values of R_{inter} are plotted in comparison with the measured TCs of various isotropic polymers and oriented polymers. R_{inter} calculated from MD of PE and PP are shown as a function of (b) interchain spacing and (c) temperature. The interchain spacings of PE and PP are 3.55 and 3.6 Å in (c), respectively.

forces between atoms in polymers, which is a general all-atom potential for the atomistic simulation of common organic molecules and polymers. The COMPASS force field predicts well the conformational energies and vibration frequencies, both closely relevant to the thermal properties of polymers [23]. The polymer models simulated by MD are purely classical systems. Therefore, we did quantum corrections to the total energy to make sure that the MD simulation temperature is equivalent to a corrected temperature at 300 K [7]. Furthermore, we simulated the MD temperature-dependent interchain resistance and found the dependence is negligible

for a fixed interchain spacing as shown in Fig. 2(c). The details of the simulations can be found in Ref. [8]. The results show that R_{inter} is sensitive on the interchain spacing, which is expected to be below 4.1 Å for PE and 4.5 Å for PP [24], as the repulsion between atoms is responsible for the thermal transport between contact chains below the glass transition temperature (T_g). The calculated R_{inter} varies from 2 to 20 K nW^{-1} and from 20 to 30 K nW^{-1} for PE and PP, respectively, when the interchain spacing varies from 3.5 to 4 Å. These values are very close to those required in Fig. 2(a), considering that the models of polymer chains in MD are oversimplified compared to the real polymers. Therefore, our model is valid and it successfully explains the origin of the small difference of TCs of polymers with completely different chemical structures. It should be pointed out that the overlap area between entangled chains is very difficult to determine. The overlap areas of the PE and PP molecular chains are taken as 4×12.7 Å^2 and 4×11 Å^2, based on their Kuhn lengths, respectively.

The temperature dependence of TC is derived from Eq. (4),

$$\frac{1}{\kappa_{am}}\frac{\partial \kappa_{am}}{\partial T} = -\frac{\alpha}{2} - \frac{\partial \ln R_{inter}}{\partial T}, \qquad (5)$$

where $\alpha = -\frac{1}{\rho}\frac{\partial \rho}{\partial T}$ is the thermal expansion coefficient. Figure 2(c) shows that R_{inter} for PE and PP weakly depend on the temperature near 300 K. When T is lower than T_g, R_{inter} would gradually decrease with decreasing temperature due to less phonon contribution. Therefore, $-\frac{\partial \ln R_{inter}}{\partial T}$ is positive at low temperature and approaches zero near room temperature. Since $-\alpha/2 < 0$, the competition between these two terms determines the temperature dependence of TC. There is a discontinuity of α at T_g [25] where their values are denoted as α_g and α_l below and above T_g, respectively (see Table II). When $T < T_g$, α_g is small and $-\frac{\partial \ln R_{inter}}{\partial T}$ is large. Taking the temperature dependence of $R_{inter} \propto T^{-\delta}$ and neglecting $-\alpha_g/2$, it is clear that TC gradually increases with temperature as

$$\frac{\kappa_{am}(T)}{\kappa_{am}(T_g)} \approx \left(\frac{T}{T_g}\right)^{\delta}, \quad T < T_g. \qquad (6)$$

This equation is consistent with the empirical formula $\frac{\kappa_{am}}{\kappa_{am}(T_g)} = \left(\frac{T}{T_g}\right)^{0.22}$ [24] when $\delta = 0.22$. When $T > T_g$, R_{inter} is almost independent of temperature, and $-\alpha_l/2$ becomes

TABLE II. Thermophysical properties of typical polymers. β of PP is measured at 453 K and others are measured around room temperature.

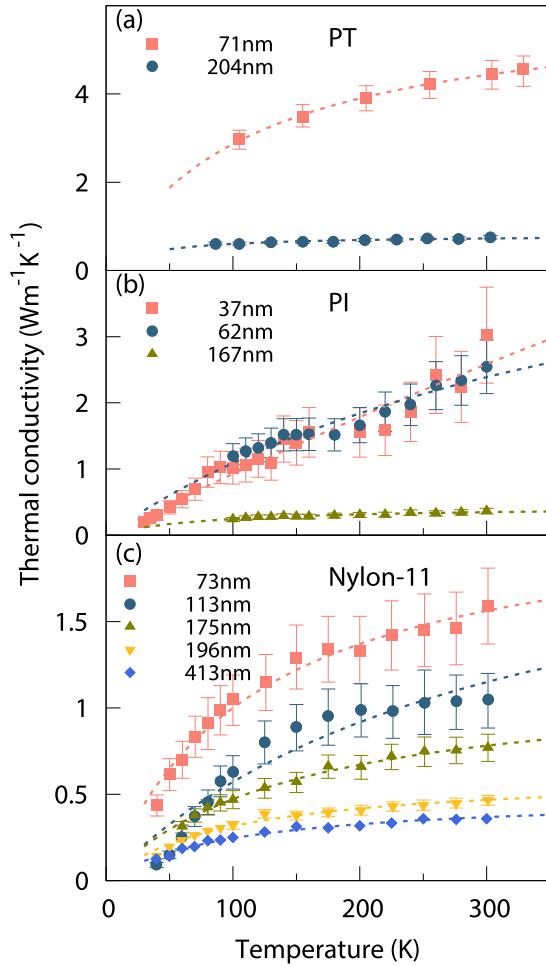| Polymers	T_g (K)	α_g (10^{-4} K^{-1})	α_l (10^{-4} K^{-1})	β (GPa^{-1})	$(1/\kappa_{am})\partial\kappa_{am}/\partial P$ (GPa^{-1})
Poly tetra fluoroethylene (PTFE)				0.36 [28]	0.1–0.9 [26]
Nylon-6 (N6)	320–330 [16]		3.4–4.0 [24]		
Poly(methyl methacrylate) (PMMA)	387 [24]	2.7 [24]	6.1–6.4 [24]	0.28 [16]	0.6–0.7 [26], 0.1–0.2 [3]
Isotactic PP	275.5 [16]	1.95 [16]	4.2 [16]	1.27 [16]	0.6 [26]
Poly(vinyl acetate) (PVAC)				0.30 [16]	0.9 [26]
Polystyrene (PS)	373 [24]	1.8–2.9 [24]	4.6–7.2 [24]	0.27 [16]	0.5 [26]
Polycarbonate (PC)	423 [16]	2.6 [16]		0.26 [16]	0.7 [26]

FIG. 3. Temperature dependence of $\kappa_\parallel$ of oriented (a) PT [12], (b) PI [14], and (c) N11 [11] with different diameters. Dots are experimental data and dashed lines are fitted by Eq. (9).

dominant, which results in a linear decrease of TC as

$$\frac{\kappa_{\rm am}(T)}{\kappa_{\rm am}(T_g)} \approx \left[\left(1 + \frac{\alpha_l T_g}{2} \right) - \frac{\alpha_l T_g}{2} \left(\frac{T}{T_g} \right) \right], \quad T > T_g. \quad (7)$$

Here, $\alpha_l T_g$ is 0.1–0.3 as shown in Table II. This is close to the empirical relation $\frac{\kappa_{\rm am}(T)}{\kappa_{\rm am}(T_g)} = 1.2 - 0.2\frac{T}{T_g}$ [24].

The pressure dependence of $\kappa_{\rm am}$ can also be derived as

$$\frac{1}{\kappa_{\rm am}} \frac{\partial \kappa_{\rm am}}{\partial P} = \frac{\beta}{2} - \frac{\partial \ln R_{\rm inter}}{\partial P}, \quad (8)$$

where $\beta = \frac{1}{\rho} \frac{\partial \rho}{\partial P}$ is the compressibility. We are not able to calculate $\frac{\partial \ln R_{\rm inter}}{\partial P}$ at the current stage. It is natural to consider that $R_{\rm inter}$ decreases with increasing pressure, due to a stronger entanglement and decreased interchain distance under pressure. Table II [26] shows that $\frac{1}{\kappa_{\rm am}} \frac{\partial \kappa_{\rm am}}{\partial P}$ is on the order of 0.1–1 GPa^{-1} and is slightly larger than $\beta/2$.

We then consider the anisotropic TC of oriented polymers. Many experiments have demonstrated that the TC along the oriented direction ($\parallel$) is much larger than $\kappa_{\rm am}$ as shown in Fig. 2(a) and Table I. The TC in the perpendicular direction ($\perp$) is smaller [27]. After orientation, $\overline{\cos\theta_\parallel} > 1/2$ and $\overline{\cos\theta_\perp} < 1/2$, where $\theta_\parallel$ and $\theta_\perp$ are the average angles of
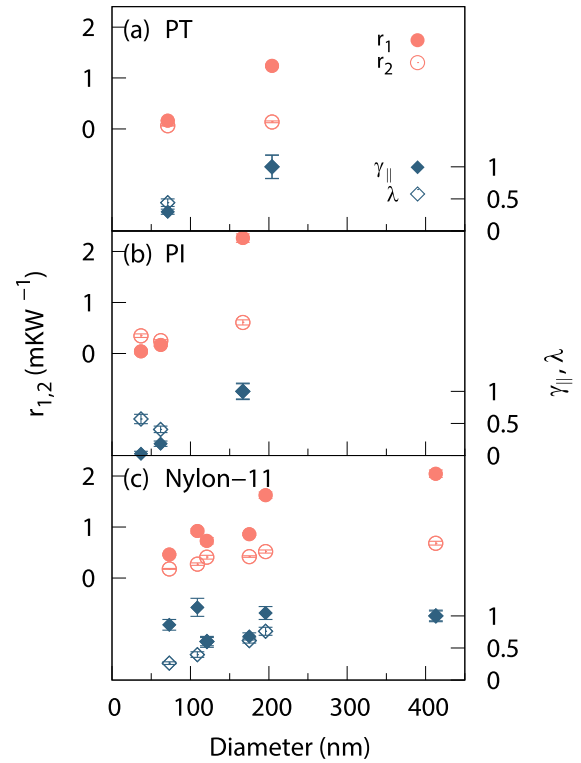
FIG. 4. The values of r_1 and r_2 vs the diameter of polymer nanofibers. $\gamma_\parallel$ and λ extracted from r_1 and r_2 are plotted in arbitrary units to the right y axis.

the chain segments with respect to the direction along and perpendicular to the orientation, respectively. The anisotropic interchain heat transfer probability ($\gamma_\parallel$) should be smaller than 1/2. Then we have

$$\kappa_\parallel = \frac{\overline{\cos\theta_\parallel}}{\xi \overline{\cos\theta_\perp}^2 [\gamma_\parallel R_{\rm inter} + (1 - \gamma_\parallel) R_{\rm intra} + R_{\rm intrin}]}. \quad (9)$$

The increase of TC is attributed to the increase of $\frac{\overline{\cos\theta_\parallel}}{\overline{\cos\theta_\perp}^2}$ and the decrease of $\gamma_\parallel$. In a highly oriented polymer, $\gamma_\parallel \ll 1$ and $\overline{\cos\theta_\parallel} \approx 1$, Eq. (9) approaches the limit as $\kappa_\parallel \to [\xi \overline{\cos\theta_\perp}^2 (R_{\rm intra} + R_{\rm intrin})]^{-1}$, which means the intrinsic TC of molecular chains is dominant and $R_{\rm inter}$ is negligible. We then take $\kappa_0 \approx \chi T$ near room temperature according to MD simulations [9] where χ is a constant. Then Eq. (9) can be simplified as $\kappa_\parallel = (r_1 + \frac{r_2}{T/T_0})^{-1}$ with two fitting parameters r_1 and r_2. Here, $r_1 = \xi \gamma_\parallel [\lambda(R_{\rm inter} - R_{\rm intra}) + R_{\rm intra}]$ and $r_2 = \frac{\xi^2 \lambda}{S\chi T_0}$, with $\lambda = \frac{\overline{\cos\theta_\perp}^2}{\overline{\cos\theta_\parallel}}$ and $T_0 = 300$ K. We fit the experimental measured $\kappa_\parallel$ of PT, PI, and N11 nanofibers with different diameters in Fig. 3. Our formula is in excellent agreement with the experimental data where the fitted r_1 and r_2 are shown in Fig. 4. It is interesting that λ and $\gamma_\parallel$ can be deduced from r_1 and r_2. For nanofibers with large diameters, r_1 is significantly larger than r_2, and then the temperature dependence of $\kappa_\parallel$ is weak, which is similar to the case of isotropic polymers. We find that both r_1 and r_2 decrease with decreasing diameter, while r_1 decreases more rapidly than r_2. This is because r_1 includes both λ and $\gamma_\parallel$ that decrease with a decrease of the diameter, while r_2 does not include $\gamma_\parallel$. As a result, r_2

becomes comparable to r_1 for diameters below 100 nm, and then $\kappa_\parallel$ shows a stronger temperature dependence. In ultrathin nanofibers with diameters smaller than 50 nm, $\frac{r_2}{T/T_0} \gg r_1$, and one can find that $\kappa_\parallel \propto T$.

Finally, we point out that our model is valid in the temperature range from several tens degrees Kelvin to the melting temperature. For temperature lower than the plateau temperature (~ 10 K), the quantum effects play a crucial role [29]. We can further extend our model to discuss other effects on TC. (1) Cross-linking effect: It is known that cross-linking could enhance the TC of amorphous polymers [30–33]. Under the framework of our model, the cross-link bonds can be seen as altering some contact points via the vdW interaction by linked points via real bonding, which will decrease $R_{\rm inter}$, thus increasing TC. (2) Branched effect: Branched polymers are found to possess a lower TC than polymers with single linear chains due to a lower density [34]. This can be easily understood that a lower density ρ results in a larger ξ, thus TC will be reduced. (3) Molecular weight: There is a relationship between the density and molecular weight of amorphous polymers, $(\rho_\infty - \rho) \propto \frac{1}{M_n}$, where ρ_∞ is the asymptotic density for a very high molecular weight and M_n is the number-averaged molecular weight [24]. Moreover, $R_{\rm inter}$ also decreases with an increasing molecular weight due to the decreased interchain distance. According to these relationships and Eq. (4), TC increases with increasing M_n and then saturates when M_n is large enough, which agrees with the experiments [35–37]. (4) TC of proteins: It is possible to apply our model for proteins by carefully taking into account the structure features of peptide chains, as proteins also possess a network structure formed by peptide chains and show similar TCs [38–40].

IV. SUMMARY

In summary, we proposed a TRN model to describe the TC of amorphous polymers. The entangled network structure and the interplay between intrachain and interchain heat transfer are considered. The fundamental mechanism of a universally low TC of polymers is attributed to the similar mean distance between contact points and the similar interchain resistance due to the vdW interaction. To summarize, our model successfully explains the temperature and pressure dependence of TC, not only in solid polymers but also in polymer melts in addition to the experimentally observed anisotropic TC.

[1] X. Xu, J. Chen, J. Zhou, and B. Li, Adv. Mater. **30**, 1705544 (2018).

[2] C. L. Choy, Polymer **18**, 984 (1977).

[3] W.-P. Hsieh, M. D. Losego, P. V. Braun, S. Shenogin, P. Keblinski, and D. G. Cahill, Phys. Rev. B **83**, 174205 (2011).

[4] X. Xie, K. Yang, D. Li, T.-H. Tsai, J. Shin, P. V. Braun, and D. G. Cahill, Phys. Rev. B **95**, 035406 (2017).

[5] S. Kommandur and S. K. Yee, J. Polym. Sci., Part B: Polym. Phys. **55**, 1160 (2017).

[6] R. Zallen, *The Physics of Amorphous Solids* (Wiley, New York, 1998), pp. 107–133.

[7] A. Henry and G. Chen, Phys. Rev. Lett. **101**, 235502 (2008).

[8] J. Liu and R. Yang, Phys. Rev. B **86**, 104307 (2012).

[9] J. W. Jiang, J. Zhao, K. Zhou, and T. Rabczuk, J. Appl. Phys. **111**, 124304 (2012).

[10] T. Lu, K. Kim, X. Li, J. Zhou, G. Chen, and J. Liu, J. Appl. Phys. **123**, 015107 (2018).

[11] Z. Zhong, M. C. Wingert, J. Strzalka, H-H. Wang, T. Sun, J. Wang, R. Chen, and Z. Jiang, Nanoscale **6**, 8283 (2014).

[12] V. Singh, T. L. Bougher, A. Weathers, Y. Cai, K. Bi, M. T. Pettes, S. A. McMenamin, W. Lv, D. P. Resler, T. R. Gattuso, D. H. Altman, K. H. Sandhage, L. Shi, A. Henry, and B. A. Cola, Nat. Nanotechnol. **9**, 384 (2014).

[13] S. Shen, A. Henry, J. Tong, R. Zheng, and G. Chen, Nat. Nanotechnol. **5**, 251 (2010).

[14] L. Dong, Q. Xi, D. Chen, J. Guo, T. Nakayama, Y. Li, Z. Liang, J. Zhou, X. Xu, and B. Li, Nat. Sci. Rev. **5**, 500 (2018).

[15] C. L. Choy, F. C. Chen, and W. H. Luk, J. Polym. Sci., Polym. Phys. Ed. **18**, 1187 (1980).

[16] J. E. Mark, *Polymer Data Handbook* (Oxford University Press, Oxford, UK, 2009).

[17] D. J. David and A. Misra, *Relating Materials Properties to Structure with MATPROP Software: Handbook and Software for Polymer Calculations and Materials Properties* (CRC Press, Boca Raton, FL, 1999), p. 531.

[18] G. D. Carvalho, E. Frollini, and W. N. D. Santos, J. Appl. Polym. Sci. **62**, 2281 (1996).

[19] N. Okui and T. Sakai, Polym. Bull. **17**, 79 (1987).

[20] K. Tashiro, K. Ono, Y. Minagawa, M. Kobayashi, T. Kawai, and K. Yoshino, J. Polym. Sci., Part B: Polym. Phys. **29**, 1223 (1991).

[21] Extracted from https://www.engineeringtoolbox.com/.

[22] C. L. Yaws, *Handbook of Thermal Conductivity*, Vol. 3 (Gulf Publishing Company, Houston, 1955).

[23] H. Sun, J. Phys. Chem. B **102**, 7338 (1998).

[24] D. W. Van Krevelen and K. Te Nijenhuis, *Properties of Polymers*, 4th ed. (Elsevier, Amsterdam, 2009), pp. 74, 92–94.

[25] R. F. Boyer and R. S. Spencer, J. Appl. Phys. **15**, 398 (1944).

[26] R. G. Ross, P. Andersson, B. Sundqvist, and G. Backstrom, Rep. Prog. Phys. **47**, 1347 (1984).

[27] Y. Lu, J. Liu, X. Xie, and D. G. Cahill, ACS Macro Lett. **5**, 646 (2016).

[28] P. Rae and D. M. Dattelbaum, Polymer **45**, 7615 (2004).

[29] P. W. Anderson, B. I. Halperin, and C. M. Varma, Philos. Mag. **25**, 1 (1972); W. A. Phillips, J. Low Temp. Phys. **7**, 351 (1972).

[30] G. Kikugawa, T. G. Desai, P. Keblinski, and T. Ohara, J. Appl. Phys. **114**, 034302 (2013).

[31] X. Xiong, M. Yang, C. L. Liu, X. B. Li, and D. W. Tang, J. Appl. Phys. **122**, 035104 (2017).

[32] V. Rashidi, E. J. Coyle, K. Sebeck, J. Kieffer, and K. P. Pipe, J. Phys. Chem. B **121**, 4600 (2017).

[33] O. Yamamoto and H. Kambe, Polym. J. **2**, 623 (1971).

[34] T. R. Fuller and A. L. Fricke, J. Appl. Polym. Sci. **15**, 1729 (1971).

[35] D. R. Anderson, Chem. Rev. **66**, 677 (1966).

[36] D. Hansen, R. C. Kantayya, and C. C. Ho, Polym. Eng. Sci. **6**, 260 (1966).

[37] J. Zhao, J.-W. Jiang, N. Wei, Y. Zhang, and T. Rabczuk, J. Appl. Phys. **113**, 184304 (2013).

[38] B. M. Foley, C. S. Gorham, J. C. Duda, R. Cheaito, C. J. Szwejkowski, C. Constantin, B. Kaehr, and P. E. Hopkins, J. Phys. Chem. Lett. **5**, 1077 (2014).

[39] J. A. Tomko, A. Pena-Francesch, H. Jung, M. Tyagi, B. D. Allen, M. C. Demirel, and P. E. Hopkins, Nat. Nanotechnol. **13**, 959 (2018).

[40] X. Yu and D. M. Leitner, J. Phys. Chem. B **107**, 1698 (2003); J. Chem. Phys. **122**, 054902 (2005).